Static, dynamic, and electronic properties of liquid gallium studied by first-principles simulation

J. M. Holender and M. J. Gillan
Physics Department, Keele University, Keele, Staffordshire ST5 5BG, United Kingdom

M. C. Payne
Cavendish Laboratory, Cambridge University, Cambridge CB3 0HE, United Kingdom

A. D. Simpson
Edinburgh Parallel Computing Centre, Edinburgh University, Edinburgh EH9 3JZ, United Kingdom
(Received 21 February 1995)

First-principles molecular-dynamics simulations having a duration of 8 ps have been used to study the static, dynamic, and electronic properties of liquid Ga at the temperatures 702 and 982 K. The simulations use the density-functional pseudopotential method and the system is maintained on the Born-Oppenheimer surface by conjugate gradients relaxation. The static structure factor and radial distribution function of the simulated system agree very closely with experimental data, but the diffusion coefficient is noticeably lower than measured values. The long simulations allow us to calculate the dynamical structure factor $S(q,\omega)$. A sound-wave peak is clearly visible in $S(q,\omega)$ at small wave vectors, and we present results for the dispersion curve and hence the sound velocity, which is close to the experimental value. The electronic density of states is very close to the free-electron form. Values of the electrical conductivity calculated from the Kubo-Greenwood formula are in satisfactory accord with measured data.

I. INTRODUCTION

Liquid gallium has been widely studied by a variety of experimental,[1–5] and theoretical methods.[6–9] The structure of the liquid is now well established over a wide range of temperatures but the knowledge of its dynamical properties, and particularly of its collective dynamics, is in a much less satisfactory state. There is also a need for a more detailed investigation of its electronic structure. In the present work, we have undertaken first-principles molecular-dynamics (MD) simulations of ℓ-Ga at two temperatures. These simulations are considerably longer than another first-principles simulation,[9] and this has allowed us to investigate the structure and electronic properties with greater statistical accuracy. More importantly, it has allowed us to investigate the dynamical structure factor, which describes the dynamics of density fluctuations.

Collective fluctuations have previously been studied in a variety of metallic and insulating liquids. Neutron-scattering experiments have shown that short-wavelength sound waves are readily observable in several liquid metals including Rb,[10] Cs,[11] and Pb.[12] In general, oscillatory fluctuations can be observed for wave vectors up to over half the wave vector of the first peak in the static structure factor. On the other hand, in some other liquids such as Ne,[13] sound waves are found to be strongly overdamped in this region of wave vectors. Classical simulations of liquid rare gases[14] and metals[15] have revealed the same qualitative difference of behavior between the two types of liquids. This difference has been traced to the fact that the short-range interatomic repulsion in simple metals is much softer than in rare gases.[16] There also seems to be a correlation with the ratio of specific heats γ, which is generally close to unity in liquid metals,[17] but is considerably greater than unity in liquid rare gases.[17] In this context, the behavior of ℓ-Ga is puzzling. Very recent inelastic neutron-scattering measurements[5] just above the melting point have failed to find oscillating density fluctuations, even though γ for ℓ-Ga has one of the lowest values among liquid metals. Here, we report first-principles simulations only at high temperatures, so that a direct comparison with the recent inelastic data cannot yet be made, but we shall show that density oscillations are clearly visible in our system. We shall suggest reasons for this apparent disagreement.

Since the work of Car and Parrinello,[18] first-principles MD simulation has become increasingly important in the study of liquids. The basic idea of the method is to calculate the total energy and the forces for any arrangement of atoms by solving the equations of density functional theory to determine the electronic ground state. The great advantages of this approach are that it completely avoids *ad hoc* assumptions about the interactions between the atoms, and that it allows the electronic properties of the liquid to be calculated within a unified framework. Simulations on ℓ-Si,[19] ℓ-GaAs,[20] ℓ-Ga,[9] ℓ-CsPb,[21] ℓ-Ge,[22] ℓ-NaSn,[23] and a number of other systems have been reported, and the structure of the simulated systems generally agrees closely with experimental data.

Another first-principle study of ℓ-Ga has been reported.[9] This was a rather short simulation at the single temperature of 1000 K, but was valuable in a number

0163-1829/95/52(2)/967(9)/$06.00

of ways. It showed that the simulated system reproduces the known structure of ℓ-Ga rather well. It also allowed an investigation of the role of covalent bonds in the liquid. Last, it gave useful insight into the electronic structure, and showed that the deep minimum in the density of states at the Fermi level known to exist in crystalline α-Ga (Ref. 7) disappears in the liquid.

The simulation technique we use differs in important ways from the one originally proposed by Car and Parrinello. We do not treat the electronic degrees of freedom as fake dynamical variables, but instead we relax the electrons to the Born-Oppenheimer surface at each time step by conjugate-gradient minimization.[24,25] This has the advantages of allowing us to use much larger time steps and also of avoiding the rather artificial use of thermostats needed for metals in the conventional Car-Parrinello technique. We also use Fermi level smoothing, treating the occupation numbers as dynamical variables, as has been done by a number of other workers.[22,24,26]

The main technical features of our simulations are explained in Sec. II. Our results for the structural, dynamical and electronic properties of ℓ-Ga are presented in Sec. III. A discussion of our findings is given in Sec. IV, and our conclusions are summarized in Sec. V.

II. TECHNIQUES

A. Method

We first summarize briefly the aspects of our simulation technique that are standard,[27] before describing in more detail the less familiar features. As usual in first-principles MD simulations, only valence electrons are explicitly represented, and it is assumed that the core states are identical to those in the free atom. In the present case, the Ga $4s$ and $4p$ electrons are counted as valence electrons, and all more tightly bound electrons are counted as part of the core. The interaction between valence electrons and the atomic cores is represented by a norm-conserving nonlocal pseudopotential, which is constructed *ab initio* via calculations on the free atom (see below for details). The calculations are performed in periodic boundary conditions, with the electronic orbitals expanded in plane waves. In this expansion, all plane waves are included whose wave vector $\boldsymbol{G}$ satisfies $\hbar^2 G^2/2m < E_{\rm cut}$ where $E_{\rm cut}$ is referred to as the plane-wave cutoff energy. The calculations can (and in principle should) be taken to convergence with respect to the size of the basis set by systematically increasing $E_{\rm cut}$. The exchange-correlation term in the density-functional expression for the total energy is represented by the local density approximation (LDA).[28] A simulation is performed by making the ions follow classical trajectories determined by the forces acting on them, while the electronic subsystem remains in the ground state at each instant (the Born-Oppenheimer principle). All these features are entirely standard.

There are two well-known problems in the first-principles MD simulation of metals. The first is that Kohn-Sham states can cross the Fermi level, so that their occupation number passes discontinuously between zero and unity. This implies that the wave-functions of occupied states can change discontinuously and that the forces on the ions can do the same. Both kinds of discontinuity can wreak havoc with the numerical implementation of the equations of motion. The second problem is that the Fermi discontinuity leads to the need for extensive (and expensive) sampling over the Brillouin zone.

It has been recognized[29] that both these problems can be solved at the same time by smearing out the Fermi discontinuity so that the occupation numbers pass continuously from unity to zero over a specified energy interval. It was also shown[24,30,31] that this idea can be formulated as a variational principle in which the quantity to be minimized has the form of a thermodynamic free energy, which depends both on the Kohn-Sham orbitals and their occupation numbers. This formulation is closely related to the Mermin density functional theory for electron systems at finite temperature.[32] The idea of working with variable occupation numbers in a free-energy framework has been expounded by a number of authors,[22,26,33] and all that is needed here is a note of some technical features peculiar to the present work.

In general, the free-energy functional can be represented as

$$A[\{\psi_i\},\{R_I\},\{f_i\}] = E[\{\psi_i\},\{R_I\},\{f_i\}] - \alpha Q(\{f_i\}) \ , \tag{1}$$

where E is the total-energy functional, which depends on the Kohn-Sham orbitals ψ_i, their occupation numbers f_i, and the ionic positions R_I; the quantity Q plays the role of an entropy, and α specifies the smearing width. In general, Q can be taken to have the form

$$Q(\{f_i\}) = 2\sum_i \zeta(f_i) \ . \tag{2}$$

If α is chosen to be $k_B T$ and $\zeta(f)$ has the form

$$\zeta(f) = -f \ln f - (1-f)\ln(1-f) \ ; \tag{3}$$

then minimization with respect to the f_i at constant electron number yields the usual Fermi-Dirac distribution

$$f_i = 1/\{\exp[(\epsilon_i - \mu)/k_B T] + 1\} \ , \tag{4}$$

where ϵ_i are the Kohn-Sham eigenvalues and μ is the chemical potential. However, it has been pointed out that many other choices of Q and hence many other equilibrium distributions for f_i are possible.[30,31] A disadvantage of the Fermi-Dirac distribution is that for a given energy width the occupation numbers f_i approach their asymptotic values of 0 and 1 rather slowly. Because of this, we prefer a distribution that approaches its asymptotic values in a Gaussian manner rather than exponentially. This is easily achieved by taking the dependence of f on ϵ to be given by

$$f(x) = \begin{cases} \frac{1}{2}\sqrt{e}\,\exp[-(x+2^{-1/2})^2] & \text{if } x > 0, \\ 1 - \frac{1}{2}\sqrt{e}\,\exp[-(x-2^{-1/2})^2] & \text{if } x < 0, \end{cases} \tag{5}$$

where

$$x = (\epsilon - \mu)/\alpha \ . \tag{6}$$

It is readily shown that this equilibrium distribution is obtained if ζ is chosen to be

$$\zeta(x) = \frac{1}{2}\sqrt{e}\,|x|\,\exp[-(|x| + 2^{-1/2})^2] + \frac{1}{4}\sqrt{\pi e}\,\mathrm{erfc}(|x| + 2^{-1/2}) \ , \tag{7}$$

where

$$x(f) = \begin{cases} [\ln(e^{1/2}/2f)]^{1/2} - 2^{-1/2} & \text{if } f < \frac{1}{2}, \\ 2^{1/2} - \{\ln[e^{1/2}/2(1-f)]\}^{1/2} & \text{if } f > \frac{1}{2}. \end{cases} \tag{8}$$

In the original Car-Parrinello method, the plane-wave coefficients were treated as fake dynamical variables. For metals, this method leads to serious problems because of the rapid transfer of energy from the ions to the electronic degrees of freedom. Because of this, we prefer to use the conjugate-gradient approach,[24,25] in which the electronic subsystem is brought to the ground state at every step. This also has the advantage of allowing one to use a much larger time step than in the standard method.

As has been stressed before,[24] with fractional occupation numbers the free energy is minimized only when the orbitals are eigenstates of the Kohn-Sham (KS) Hamiltonian. This is to be contrasted with the situation for insulators, where it suffices that the orbitals span the occupied subspace. Because of this, it is essential to perform explicit subspace rotation so as to make the orbitals eigenstates. The procedure we use for this is essentially the same as that of Gillan,[24] which is closely related to the methods described subsequently by Grumbach *et al.*[26] and Kresse and Hafner.[22]

Briefly, the above features of our technique are implemented by the following strategy which is based on Ref. 24. The occupation numbers and wave-function coefficients are varied together and we minimize all bands simultaneously. We apply the standard conjugate-gradient technique to the wave-function coefficients. For occupation numbers we apply a simpler method. At a given iteration we have occupation numbers $\{f_i\}$. These are used to calculate the "electronic forces" and the KS Hamiltonian. From the diagonal elements of the KS Hamiltonian we calculate new occupation numbers $\{\tilde{f}_i\}$. The changes in the occupation numbers are made according to

$$f_i' = f_i + \gamma\,(\tilde{f}_i - f_i) \ . \tag{9}$$

The free energy A is bound to decrease for some positive value of γ. This change is made simultaneously with the standard conjugate-gradient step and is followed by subspace rotation.[24] This cycle is repeated until the change in the free energy during one cycle is smaller than some tolerance.

Special attention has to be paid to bands above the Fermi level, which have low occupation numbers. These influence the total energy in two ways: directly and indirectly. The direct influence comes from the explicit appearance of wave functions of weakly occupied bands in the total energy. The indirect influence arises from projection of forces and subspace rotation. Weakly occupied bands should not be allowed to vary in an uncontrolled manner and it is highly desirable that they should be close to the KS eigenstates. There are always a few bands with very small occupation number and their direct contribution to the total free-energy is almost negligible. Since our algorithm is based on free energy minimization, normal conjugate gradients will have great difficulty in bringing these bands close to KS eigenfunctions. To achieve this, we must use preconditioning. We work with scaled wave-function coefficients. We find that scaling of all wave-function coefficients by the factor $f_i^{1/2}$ solves problems with weakly occupied bands.

The calculations have been done partly with the CASTEP code[25] on the Fujitsu VPX240 at Manchester, and partly with its parallel version CETEP (Ref. 34) on the CRAY T3D at Edinburgh. The codes have been extensively rewritten, partly to allow all-bands operation, in which all bands are updated simultaneously during the conjugate-gradient search, and partly to introduce the variable occupation number technique described above.

B. Computational details

The norm-conserving pseudopotential for Ga was constructed using the standard Kerker[35] method, the s and p components being generated from the neutral $4s^2 4p^1$ configuration and the d component from the ionized $4s^{0.75}4d^{0.25}$ configuration. In the practical calculations, the pseudopotential is represented in the Kleinman-Bylander separable form[36] with the s wave being treated as local, and the nonlocal parts of the pseudopotential being treated in real space.[37] In the construction of the pseudopotential and in the simulations, the exchange-correlation energy is represented in the Ceperley-Alder form.[28]

We have tested the pseudopotential by calculations on the α phase of crystalline Ga. This is the stable crystal structure under ambient conditions, and has a based-centered orthorhombic Bravais lattice with eight atoms in the unit cell. In order to achieve high accuracy, we have used the rather large plane-wave cutoff of 250 eV and a set of 32 k points. The calculated values of lattice parameters were 4.37 Å, 4.38 Å, 7.42 Å, and the internal parameters were 0.07 and 0.16. The corresponding experimental values are 4.511 Å, 4.517 Å, 7.645 Å and 0.078 and 0.1525.[38] The main deficiency of the calculations is clearly the error of ca. 3% in the lattice parameters. Essentially the same error was reported by Gong *et al.*[39] and we believe it arises from the LDA approximation. In all our calculations for the liquid we accept that we are bound to make this error and all distances are scaled accordingly when comparison with experimental data is made.

Our calculations on ℓ-Ga were all performed on a system of 64 Ga atoms using a cubic repeating cell, with the

density equal to the experimental value at each temperature with the above-mentioned scaling of distances. The plane-wave cutoff for the liquid simulations was taken to be 125 eV, and Γ-point sampling was used in the calculation of the (free) energy and the forces at each time step. The Verlet algorithm was used to integrate the equations of motion for the atomic positions and velocities, with a time step Δt of 3 fs. As explained above, the number of bands has to be taken greater than half the number of valence electrons, in order to allow for partial occupation. We worked with 102 bands, which is 6 more than would be needed for the 192 valence electrons if all bands were fully occupied. The smearing width [the parameter α in Eq. (6)] was equal to 0.2 eV.

We initiated the system at 1000 K. We equilibrated our system for about 10 ps at this temperature and then we collected data over 8 ps. The average temperature was 982 K. Then the system was slowly cooled at the rate 40 K ps^{-1} until the temperature of 700 K was reached. This was followed by a further run of 8 ps at 700 K, the average temperature in this run being 702 K.

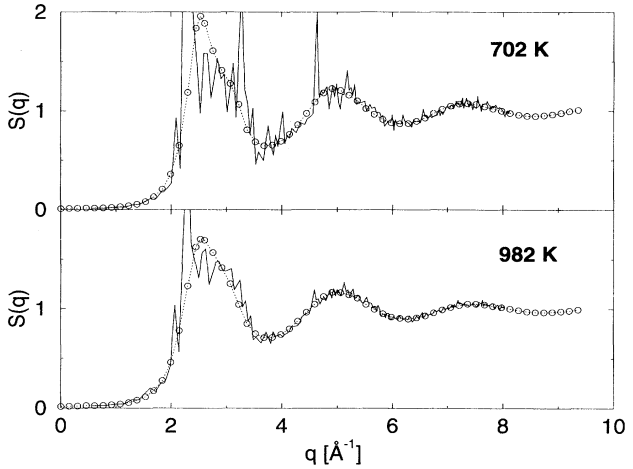

FIG. 1. The static structure factor $S(q)$ of ℓ-Ga at 702 and 982 K. Solid line and circles connected by dotted line represent simulation and experimental values (Ref. 1), respectively.

III. RESULTS

A. Structural properties

The structure of the simulated liquid can be compared directly with that of the real system through the static structure factor $S(q)$, which is measured in diffraction experiments. This quantity is a measure of the intensity of density fluctuations as a function of wave vector $\mathbf{q}$, and is defined by

$$S(q) = \langle |\hat{\rho}(\boldsymbol{q})|^2 \rangle \ . \tag{10}$$

Here the dynamical variable $\hat{\rho}(\boldsymbol{q})$ representing the Fourier component of the atomic density at wave vector $\boldsymbol{q}$ is given by

$$\hat{\rho}(\boldsymbol{q}) = N^{-1/2} \sum_{i=1}^{N} \exp(i\boldsymbol{q} \cdot \boldsymbol{r}_i) \ , \tag{11}$$

where $\boldsymbol{r}_i$ is the position of atom i and N is the number of atoms in the system. The angular brackets in Eq. (10) denote the thermal average, which in practice is evaluated as the time average over the duration of the simulation. In practical calculations of $S(q)$, we also average over $\boldsymbol{q}$ vectors having the same magnitude.

Our results for $S(q)$ at 702 K and 982 K are compared in Fig. 1 with the neutron-diffraction data of Bellissent-Funel *et al.*[1] We note that the latter data differ substantially from the other results cited in the compilation by Waseda,[40] which appear to be much less reliable. The measurements in Ref. 1 were performed only at 329 K and 956 K. Our results at 982 K are compared directly with the experimental data at 956 K, but to make comparison at 702 K we have used a linear interpolation of the experimental values at 329 and 956 K. The small size of our simulated system places a rather strong limitation on the wave-vector resolution of our results, and this is partly responsible for their spiky form in the region of the first peak. This feature is also present in previous first-principles simulations of liquids (see, e.g., Refs. 9, 19, 20). Allowing for this, the agreement between the simulated and experimental structure factors is close, particularly away from the first peak. The period, amplitude, and phase of the oscillations beyond ca. 4 Å^{-1} are very well reproduced.

It is also interesting to consider the low-q limit of $S(q)$, which is related to the bulk isothermal compressibility χ_T by the relation

$$S(q \to 0) = nk_B T \chi_T \ , \tag{12}$$

where n is the number density. From an extrapolation of our low-q results at 702 K, we obtain the estimate $S(q \to 0) \approx 0.012$, which gives $\chi_T = 2.4 \times 10^{-11}$ m^2 N^{-1}. This agrees fairly closely with the experimental value for the adiabatic compressibility[4] χ_S which is 2.2×10^{-11} m^{2}N^{-1}. As $\chi_T/\chi_S = C_p/C_v = \gamma$ and for ℓ-Ga this value is[17] 1.1 the above comparison of the isothermal and adiabatic compressibilities is well justified. We shall return to the elastic properties of the liquid when we discuss sound waves in Sec. III B.

The structure of the liquid can be seen more clearly from the radial distribution function $g(r)$, and we compare simulated and experimental[1] results at 702 K and 982 K in Fig. 2. As before, the "experimental" curve is obtained by interpolation. The close agreement between simulation and experiment in the region of the first peak reflects the closeness of the structure factors beyond ca. 4 Å^{-1}. There are, however, slight discrepancies between the $g(r)$ values beyond the first peak, and the reality of these discrepancies is confirmed by the fact that they have the same form at 702 K and 982 K. Since this region of r is associated with the first peak of the structure factor, where we have suggested an effect of system size, it

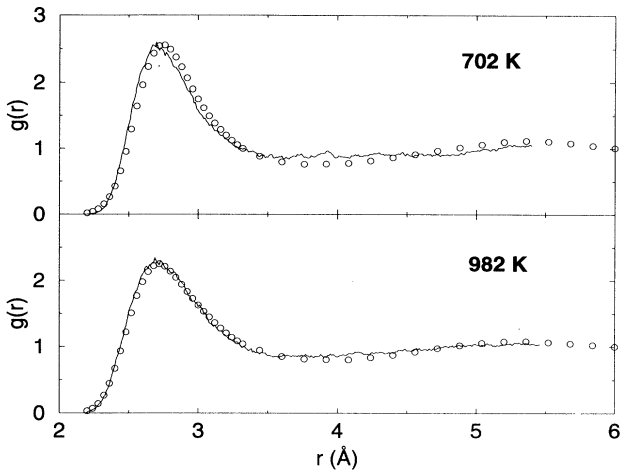

FIG. 2. The radial distribution function $g(r)$ of ℓ-Ga at 702 and 982 K. Solid line and circles represent simulation and experimental results (Ref. 1), respectively.

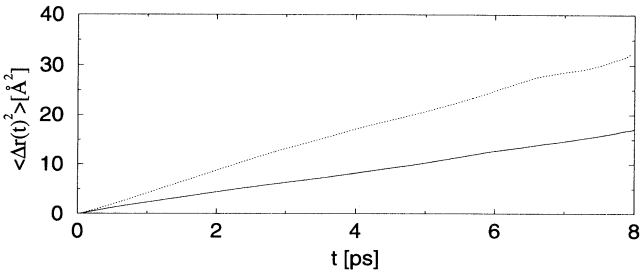

FIG. 3. Time-dependent mean square displacement $\langle \Delta r(t)^2 \rangle$ for ℓ-Ga calculated from simulations at 702 K (solid line) and 982 K (dotted line).

may well be that the small size of the system is responsible for the discrepancies.

We have calculated the average coordination number defined in the usual way as the average number of atoms within a distance r_c of a given atom, where r_c is the distance at which $g(r)$ has its first minimum. Our calculated values at 702 K and 982 K are 8.7 and 9.1, respectively. These values are essentially the same as the value of 9 that has been deduced from experimental measurements,[1] as would be expected from the close agreement between the simulated and experimental $g(r)$. The coordination numbers in the crystalline α and β phases are 7 and 8, respectively, so that there is a small but significant increase on going from solid to liquid. This is expected from the density increase on melting.[17]

B. Dynamical properties

In order to study how the atoms diffuse in the liquid, we have calculated the time-dependent mean square displacement (MSD) which we denote by $\langle \Delta r(t)^2 \rangle$. For a large time interval t, the asymptotic form of the MSD is expected to be

$$\langle \Delta r(t)^2 \rangle \rightarrow B + 6\,D\,|t| \ , \tag{13}$$

where B is a constant and D is the tracer diffusion coefficient. In calculating the MSD, we average in the usual way over all atoms in the system and over time origins. The interval between the origins is taken as Δt, so that every step serves as an origin.

Our results for the MSD at 702 K and 982 K displayed in Fig. 3 show that the atoms are diffusing rapidly, as expected. For example, the plots show that at 982 K the typical time taken for an atom to travel the nearest neighbor distance of 2.7 Å is roughly 1.5 ps. As usually happens in highly mobile liquids, the MSD rapidly reaches its asymptotic linear behavior, the transient time being roughly 0.1 ps. From the asymptotic slope of the MSD we obtain values for the diffusion coefficient of 3.3×10^{-5} and $6.5 \times 10^{-5}\,\mathrm{cm^2\,s^{-1}}$ at 702 and 982 K, respectively. These are considerably smaller than the rather old experimental values of 9×10^{-5} and $1.3 \times 10^{-4}\ \mathrm{cm^2\ s^{-1}}$ at these temperatures.[2] We discuss later the significance of these discrepancies.

The MSD is a single-particle correlation function. It is also of considerable interest to examine the collective dynamics of density fluctuations in the liquid, characterized by the intermediate scattering function $I(q,t)$, and its Fourier transform, the dynamical structure factor $S(q,\omega)$. The latter quantity is important because it can be measured rather directly by inelastic neutron scattering, and such measurements have recently been reported for ℓ-Ga.[5] The intermediate scattering function is defined as

$$I(\boldsymbol{q},t) = \left\langle \hat{\rho}(\boldsymbol{q},t) \cdot \hat{\rho}(-\boldsymbol{q},0) \right\rangle \ , \tag{14}$$

where $\hat{\rho}(\boldsymbol{q})$ is the Fourier component of the density, as before. Note that $I(\boldsymbol{q},t)$ is a real quantity which in an isotropic liquid depends only on the *magnitude* of $\mathbf{q}$.

We have calculated $I(q,t)$ directly from its definition, averaging both over time origins and over the orientation of $\mathbf{q}$. The interval between time origins was taken to be Δt. Our results for a range of wave vectors at 702 and 982 K are shown in Fig. 4. The very similar form of the plots for the two temperatures confirms that the simulation runs are long enough to be statistically reliable. Note that at $t = 0$, $I(q,t)$ becomes identical to the static structure factor $S(q)$, so that the systematic difference between the zero-time values at the two temperatures simply reflects the temperature dependence of $S(q)$, which we have already noted in Fig. 1. The most significant feature of $I(q,t)$ is the pronounced oscillations observed at low q, which rapidly become overdamped for $q > 1.8\,\mathrm{Å^{-1}}$. These oscillations represent sound waves, as we shall see immediately.

The power spectrum of density fluctuations is described by the dynamical structure factor defined by

$$S(q,\omega) = \frac{1}{\pi} \int_0^\infty \cos(\omega\, t)\, I(q,t)\, dt \ . \tag{15}$$

We have performed the transformation using the Welch

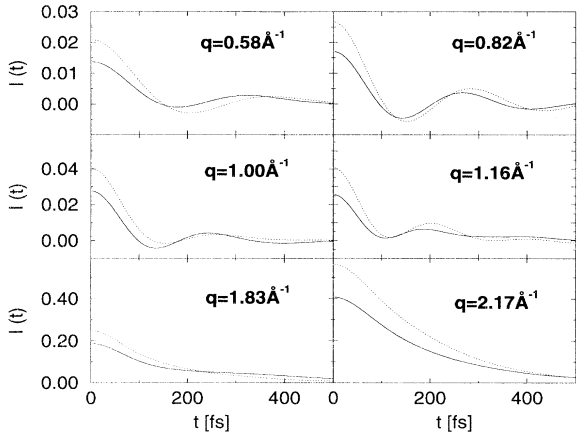

FIG. 4. The intermediate scattering function $I(q,t)$ for ℓ-Ga calculated at 702 K (solid line) and 982 K (dotted line) for six different wave vectors q.

window function[41] cutting off at maximum time 1 ps. Our results for $S(q,\omega)$ shown in Fig. 5 reveal two main features: a peak centered at zero frequency representing decaying fluctuations and a finite-frequency peak representing oscillations. These features have been observed many times before both in classical MD simulations of liquids and in inelastic scattering experiments. At small wave vectors, the central peak is associated with heat diffusion, but at the wave vectors we are dealing with here its interpretation becomes more complicated.[16] As we have already seen from $I(q,t)$, the oscillatory fluctuations survive only for wave vectors up to 1.8 Å^{-1}, beyond which we are left only with the central peak.

Our results for $S(q,\omega)$ can be used to construct a dispersion curve for sound waves in the range of q for which they can be observed. To do this, for each q we have taken the frequency $\omega_{\max}$ at which the sound-wave peak in $S(q,\omega)$ has its maximum. Figure 6 shows plots of $\omega_{\max}$ against q, on which we have superimposed straight lines whose slope is equal to the experimental adiabatic sound velocity in ℓ-Ga.[4] We note that the shape of our dispersion curve is very similar to experimental dispersion curves found for Rb,[10] Cs,[11] and Pb.[12]

Note that a linear dispersion curve is expected only in the asymptotic region of small q where the wavelength is greater than all other relevant lengths. The form of our dispersion curve indicates that the lowest two of the wave vectors available to us are within this region to sufficient accuracy, so that we are justified in making a comparison with the measured sound velocity. It is not entirely clear whether the dispersion curve we observe should be associated with adiabatic or isothermal fluctuations. Strictly speaking, sound waves are adiabatic only at wave vectors for which the sound-wave frequency is much greater than the width of the Rayleigh peak, and this is not obviously true in the present case. However, we have already pointed that the isothermal and adiabatic compressibilities should not differ more than 10% in ℓ-Ga, and this suggests a difference of the isothermal and adiabatic sound velocities of only 5%. Our conclusion is that the good agreement of our dispersion curve with the measured sound velocity is genuine. Close agreement is, of course, not unexpected, since we saw in Sec. III A that the compressibility of the simulated system accords well with the known value.

C. Electronic properties

One of the important questions about ℓ-Ga is the extent to which it can be considered a free-electron metal. The most direct way of studying this question is through the electronic density of states (DOS), since deviations of this quantity from the free-electron form are immediately apparent. It is well established that the DOS

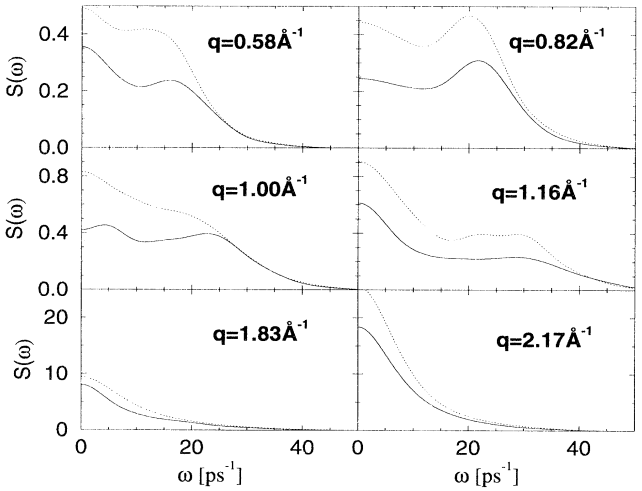

FIG. 5. The dynamical structure factor $S(q,\omega)$ for ℓ-Ga calculated at 702 K (solid line) and 982 K (dotted line) for six different wave vectors q.

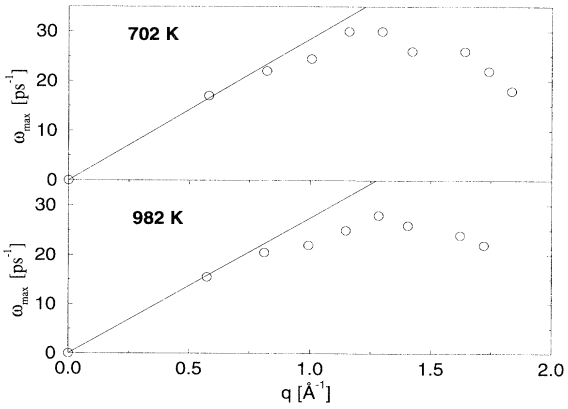

FIG. 6. The dispersion curve for sound waves in ℓ-Ga at 702 and 982 K. Circles represent frequencies $\omega_{\max}$ at which $S(q,\omega)$ of the simulated system has its peak value. The straight line represents the experimental sound-wave velocity (Ref. 4) at each temperature.

in crystalline α-Ga shows a deep minimum at the Fermi energy,[7] and it is of interest to know whether this feature survives in the liquid.

It is important to recognize that adequate k-point sampling is essential in calculating the DOS. In the first-principles MD simulations themselves, Γ-point sampling is used in the calculation of the total energy and the forces, but the direct use of the Kohn-Sham eigenvalues at the Γ point would not be satisfactory for calculating the DOS. Our procedure is to select a number of configurations from the simulation run, and for each one we have used the Kohn-Sham Hamiltonian generated in the simulation to calculate the electronic eigenvalues at a set of k points. The DOS is then obtained by averaging over configurations and k points. The k-point set we have used consists of the eight points $(\frac{1}{8},\frac{1}{8},\frac{1}{8})$, $(\frac{1}{8},\frac{1}{8},\frac{3}{8})$, $(\frac{1}{8},\frac{3}{8},\frac{3}{8})$, $(\frac{3}{8},\frac{3}{8},\frac{3}{8})$ and cyclic permutations; the points are taken with equal weights. Tests with other k points indicate that this k-point set is perfectly adequate. We have also tested explicitly the effect of calculating the DOS with Γ-point sampling only, and we find that this produces large spurious minima at certain energies. We have found that good statistical accuracy is already obtained with a fairly small number of configurations, and our results were obtained by averaging over five configurations at each temperature.

We display in Fig. 7 our calculated electronic DOS at 702 and 982 K together with the free-electron curve. It is clear that deviations from the free-electron form are very small in both cases, and there is no trace of the deep minimum at the Fermi level characteristic of the α-Ga structure. This conclusion agrees with the findings of Hafner and Jank[7] which were based on perturbation theory arguments, but does not agree well with the first-principles MD results of Gong *et al.*,[9] which show quite strong deviations from free-electron behavior. We believe that this discrepancy is due to the inadequate k-point sampling used by Gong *et al.* as we discuss later.

We have calculated the frequency-dependent electrical conductivity $\sigma(\omega)$ from the Kubo-Greenwood formula

$$\sigma(\omega) = \frac{2\pi e^2}{3m^2\omega\Omega} \sum_{i}^{\text{occup}} \sum_{j}^{\text{empty}} \sum_{\alpha=x,y,z} |\langle\psi_i|\hat{p}_\alpha|\psi_j\rangle|^2 \times\delta(E_j - E_i - \hbar\omega) \ , \tag{16}$$

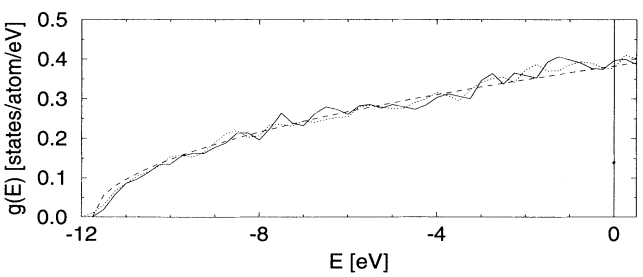

FIG. 7. Electronic density of states of ℓ-Ga calculated from simulations at 702 K (solid line) and 982 K (dotted line) compared with the free-electron form (dashed line). The vertical line denotes the Fermi energy.

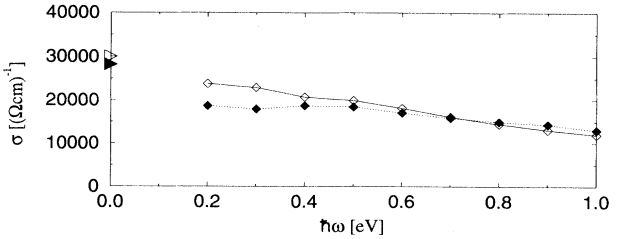

FIG. 8. Frequency-dependent electrical conductivity $\sigma(\omega)$ of ℓ-Ga calculated from simulations at 702 K (open diamonds connected by solid line) and 982 K (solid diamonds connected by dotted line). Open and solid triangles show experimental values of dc conductivity (Ref. 3) at the two temperatures.

where ψ_i and ψ_j are the wave-functions of states below and above the Fermi level, respectively, and E_i, E_j are the corresponding eigenvalues. The operator $\hat{p}_\alpha$ represents the momentum of an electron in Cartesian direction α, and Ω is the volume of the simulation cell. This is an approximate formula, which treats the valence electrons as propagating independently of one another. As in the calculations of the DOS, Brillouin-zone sampling is important, and we have used the same k-point set as for the DOS. Averaging is performed over 5 configurations at each temperature.

We show our calculated $\sigma(\omega)$ in Fig. 8. Our main interest is in the dc conductivity and we have included unoccupied states only up to 1 eV above the Fermi level. This means that $\sigma(\omega)$ is correctly calculated only for frequencies $\hbar\omega \leq 1$ eV. It should be noted that the statistical accuracy deteriorates as ω goes to zero, but this does not prevent us from making a reasonably reliable extrapolation to the dc value. Our estimates for $\sigma(0)$ at 702 K and 982 K are $2.5 \times 10^4\,\Omega^{-1}\,\text{cm}^{-1}$ and $2.0 \times 10^4\,\Omega^{-1}\,\text{cm}^{-1}$. The corresponding experimental values[3] are $3.0 \times 10^4\,\Omega^{-1}\,\text{cm}^{-1}$ and $2.8 \times 10^4\,\Omega^{-1}\,\text{cm}^{-1}$, respectively.

IV. DISCUSSION

Our first-principles simulations of ℓ-Ga are considerably longer than the only previous simulation reported so far,[9] and we have been able to study its static, dynamic, and electronic properties in more detail than before. Our comparisons of the static structure factor $S(q)$ and the radial distribution function $g(r)$ at 702 and 982 K with experimental data have confirmed that the structure of the simulated system agrees closely with that of the real liquid. However, we have found noticeable discrepancies which appear as spikes in $S(q)$ at certain wave vectors in the simulated system. This effect is stronger at the lower temperature, and discrepancies between the simulated and experimental $g(r)$ are also more significant at this temperature, though it should be remembered that the experimental $g(r)$ at 702 K is actually obtained by a rather large interpolation. We have suggested that the spikes we find in $S(q)$ are associated with the rather small size of our system, and we note that similar effects have

been seen in other first-principles simulations. It would clearly be desirable to check this point by repeating the simulations on larger systems, but we are not in a position to do this at present.

Our results for the MSD $\langle \Delta r(t)^2 \rangle$ show typical liquid-like behavior, with the asymptotic linear regime being reached after only ~ 0.1 ps. The values of the diffusion coefficient obtained from the asymptotic slope of the MSD appear to be somewhat low compared with the rather limited and old experimental data. The highest temperature at which we can make a direct comparison is 702 K, where our simulated value appears to be too low by a factor of ~ 2.7. An extrapolation of the experimental values suggests that at 980 K our simulated result is too low by a factor of ~ 2. There are two possible explanations for this. Either the experimental data are unreliable, or the simulations are suffering from a systematic error. If one wished to take the latter point of view, one would note that the spikes in $S(q)$ are indicative of a spurious ordering, which might have the effect of suppressing the atomic diffusion. This again points to the desirability of studies on larger systems. At the same time, we believe there would be a case for repeating the experimental measurements, before deciding that the simulations are at fault.

Our investigations of the collective dynamics of ℓ-Ga have shown that density oscillations are clearly visible for wave vectors $q \leq 1.5$ Å^{-1}, both directly through the oscillations in $I(q,t)$ and through the finite-frequency peaks in $S(q,\omega)$. We have shown that the dispersion curves obtained from these peaks give a small-q slope that agrees very closely with the experimental sound velocity. This observation is not at all surprising, given the well-established density oscillations in other liquid metals in the corresponding wave-vector range. However, it raises important questions about the behavior of ℓ-Ga, since Bermejo *et al.*[5] failed to observe density oscillations in ℓ-Ga at just above the melting point (actually at 330 K) using inelastic neutron scattering. We believe that the key to this apparent disagreement lies in the large difference of temperatures employed in the neutron-scattering measurements and in our simulations. It would be expected that the shear and longitudinal viscosities would increase with decreasing temperature, so that sound waves would be more heavily damped at lower temperatures. Unfortunately, there seems to bo no experimental information on the temperature dependence of the viscosities in ℓ-Ga, but we note that an increase of the viscosities with decreasing temperature would be generally consistent with the known decrease of diffusion coefficient at lower temperatures. It is plausible that such an increase of viscosity at low temperatures would lead to overdamping of sound waves in the wave vector range observable by neutron scattering. We frankly admit that this explanation is speculative. Resolution of this question clearly requires either extension of the experiments to higher or extension of the simulations to lower temperatures.

Our calculations of the DOS demonstrate that the electronic structure is close to being free-electron-like at both temperatures studied. In fact, our calculated DOS is much closer to the free electron form than the DOS reported by Gong *et al.*[9] There is an important technical point here. As we have emphasized, completely erroneous results for the DOS are obtained if adequate sampling over the Brillouin zone is not performed, a point which has been made before Kresse and Hafner.[22] But Gong *et al.* report that they have calculated the DOS using Γ-point sampling only, and we believe that this must cast serious doubt on their results. We note that the close agreement between the electronic DOS and the free-electron form provides strong support for Hafner's perturbation theory approach,[7] in which the structure of ℓ-Ga and other metals has been treated by expanding the total energy of the system to second order in the pseudopotential starting from the free-electron gas. The satisfactory agreement of our calculated dc conductivity with experimental values — the 20% discrepancy that we find is rather typical of what has been found in previous first-principles work — provides useful confirmation that the electronic structure of our simulated system is close to that of the real liquid.

V. CONCLUSIONS

In conclusion, we have performed first-principles MD simulations of ℓ-Ga at two high temperatures. The static structure of the simulated system agrees closely with that of the real liquid, but there are slight discrepancies which may arise from the small size of the simulated system. The diffusion coefficient of the simulated system appears to be too low by somewhat over a factor of 2. Oscillating density fluctuations are clearly visible, the associated sound velocity being in excellent accordance with the known value. The failure to observe sound waves in earlier neutron-scattering experiments at just above the melting point may be due to the much higher viscosity at low temperatures. The electronic DOS is very close to the free-electron form, and the calculated dc conductivity is in satisfactory agreement with experiment.

ACKNOWLEDGMENTS

The work of J.M.H. is supported by EPSRC Grant No. GR/H67935. The computations were performed partly on the Fujitsu VPX240 at Manchester Computer Centre under EPSRC Grant No. GR/J69974, and partly on the Cray T3D at Edinburgh Parallel Computer Centre using an allocation of time from the High Performance Computing Initiative to the U.K. Car Parrinello consortium. Analysis of the results was performed using distributed hardware provided under EPSRC Grant Nos. GR/H31783 and GR/J36266. We are grateful to Dr. M. C. Bellissent-Funel for sending us the numerical results of the neutron measurements of the structure of liquid gallium. Useful technical assistance from Dr. I. Bush at EPSRC Daresbury Laboratory is gratefully acknowledged.

[1] M. C. Bellissent-Funel, P. Chieux, D. Levesque, and J. J. Weis, Phys. Rev. B **39**, 6310 (1989).
[2] E. F. Broome and H. A. Walls, Trans. Met. AIME **245**, 739 (1969).
[3] G. Ginter, J. G. Gasser, and R. Kleim, Philos. Mag. B **54**, 543 (1986).
[4] M. Inui, S. Takeda, and T. Uechi, J. Phys. Soc. Jpn. **61**, 3203 (1992).
[5] F. J. Bermejo, M. García-Hernández, J. L. Martinez, and B. Hennion, Phys. Rev. E **49**, 3133 (1994).
[6] J. Hafner and G. Kahl, J. Phys. F **14**, 2259 (1984).
[7] J. Hafner and W. Jank, Phys. Rev. B **42**, 11530 (1990).
[8] S. F. Tsay and S. Wang, Phys. Rev. B **50**, 108 (1994).
[9] X. G. Gong, G. L. Chiarotti, M. Parrinello, and E. Tosatti, Europhys. Lett. **21**, 469 (1993).
[10] J. R. D. Copley and J. M. Rowe, Phys. Rev. Lett. **32**, 49 (1974).
[11] T. Bodensteiner, Chr. Morkel, W. Gläser, and B. Dorner, Phys. Rev. B **45**, 5709 (1992).
[12] O. Söderström, J. R. D. Copley, J.-B. Suck, and B. Dorner, J. Phys. F **10**, L151 (1980).
[13] H. Bell, H. Moeller-Wenghoffer, A. Kollmar, R. Stockmeyer, T. Springer, and H. Stiller, Phys. Rev. A **11**, 316 (1975).
[14] D. Levesque, L. Verlet, and J. Kürkijarvi, Phys. Rev. A **7**, 1690 (1973).
[15] A. Rahman, Phys. Rev. Lett. **32**, 52 (1974).
[16] J.-P. Hansen and I. R. McDonald, *Theory of Simple Liquids* (Academic Press, London, 1986).
[17] T. E. Faber, *Introduction to the Theory of Liquid Metals* (Cambridge University Press, Cambridge, England, 1972).
[18] R. Car and M. Parrinello, Phys. Rev. Lett. **55**, 2471 (1985).
[19] I. Štich, R. Car, and M. Parrinello, Phys. Rev. Lett. **63**, 2240 (1989).
[20] Q. M. Zhang, G. Chiarotti, A. Selloni, R. Car, and M. Parrinello, Phys. Rev. B **42**, 5071 (1990).
[21] G. A. de Wijs, G. Pastore, A. Selloni, and W. van der Lugt, Europhys. Lett. **27**, 667 (1994).
[22] G. Kresse and J. Hafner, Phys. Rev. B **49**, 14251 (1994).
[23] M. Schöne, R. Kaschner, and G. Seifert, J. Phys. Condens. Matter **7**, L19 (1995).
[24] M. J. Gillan, J. Phys. Condens. Matter **1**, 689 (1989).
[25] M. C. Payne, M. P. Teter, D. C. Allan, T. A. Arias, and J. D. Joannopoulos, Rev. Mod. Phys. **64**, 1045 (1992).
[26] M. P. Grumbach, D. Hohl, R. M. Martin, and R. Car, J. Phys. Condens. Matter **6**, 1999 (1994).
[27] For reviews of the general methods used here, see, e.g., G. P. Srivastava and D. Weaire, Adv. Phys. **36**, 463 (1987); J. Ihm, Rep. Prog. Phys. **51**, 105 (1988); M. J. Gillan, in *Computer Simulation in Materials Science*, edited by M. Meyer and V. Pontikis (Kluwer, Dordrecht, 1991), p. 257; G. Galli and M. Parinello, in *ibid.* p. 283.
[28] D. M. Ceperley and B. Alder, Phys. Rev. Lett. **45**, 566 (1980); J. Perdew and A. Zunger, Phys. Rev. B **23**, 5048 (1981).
[29] C.-L. Fu and K.-M. Ho, Phys. Rev. B **28**, 5480 (1983).
[30] M. J. Gillan, in *Rapport d'Activité du CECAM*, edited by C. Moser (CECAM, Paris, 1988).
[31] A. De Vita, Ph.D. thesis, Keele University, 1992.
[32] N. D. Mermin, Phys. Rev. A **137**, 1441 (1965).
[33] R. M. Wentzcovitch, J. L. Martins, and P. B. Allen, Phys. Rev. B **45**, 11372 (1992).
[34] L. J. Clarke, I. Štich, and M. C. Payne, Comput. Phys. Comm. **72**, 14 (1992).
[35] G. P. Kerker, J. Phys. C **13**, L189 (1980).
[36] L. Kleinman and D. M. Bylander, Phys. Rev. Lett. **48**, 1425 (1982).
[37] R. D. King-Smith, M. C. Payne, and J. S. Lin, Phys. Rev. B **44**, 13063 (1991).
[38] R. W. G. Wyckoff, *Crystal Structures*, 2nd ed. (Interscience, New York, 1964), Vol. 1.
[39] X. G. Gong, G. L. Chiarotti, M. Parrinello, and E. Tosatti, Phys. Rev. B **43**, 14277 (1991).
[40] Y. Waseda, *Structure of Non-Crystalline Materials* (McGraw-Hill, New York, 1980).
[41] W. H. Press, S. A. Teukolsky, W. T. Vetterling, and B. P. Flannery, *Numerical Recipes* (Cambridge University Press, Cambridge, England, 1992).